

Transforming growth factor- $\!\beta\!$ in the pathogenesis of breast cancer metastasis and fibrosis

Petersen, Maj

Citation

Petersen, M. (2010, June 30). *Transforming growth factor-β in the pathogenesis of breast cancer metastasis and fibrosis*. Retrieved from https://hdl.handle.net/1887/15749

Version: Corrected Publisher's Version

License: License agreement concerning inclusion of doctoral thesis in the

Institutional Repository of the University of Leiden

Downloaded from: https://hdl.handle.net/1887/15749

Note: To cite this publication please use the final published version (if applicable).

Chapter 2

Smad2 and Smad3 have opposing roles in breast cancer bone metastasis by differentially affecting tumor angiogenesis

Maj Petersen*, Evangelia Pardali*, Geertje van der Horst[†], Henry Cheung[†], Christel van den Hoogen[†], Gabri van der Pluijm^{†,§1}, and Peter ten Dijke*

*Department of Molecular Cell Biology and Centre for Biomedical Genetics, †Urology and §Endocrinology, Leiden University Medical Center, The Netherlands.

Published in *Oncogene* December 2009.

¹To whom correspondence should be addressed e-mail: G.van_der_Pluijm@lumc.nl

Abstract

Transforming growth factor (TGF)- β can suppress and promote breast cancer progression. How $TGF-\beta$ elicits these dichotomous functions and which roles the principle intracellular effector proteins Smad2 and Smad3 have therein, is unclear. Here we investigated the specific functions of Smad2 and Smad3 in TGF-β-induced responses in breast cancer cells in vitro and in a mouse model for breast cancer metastasis. We stably knocked down Smad2 or Smad3 expression in MDA-MB-231 breast cancer cells. The TGF- β -induced Smad3-mediated transcriptional response was mitigated and enhancedby Smad3 and Smad2 knockdown, respectively. This response was also seen for TGF-βinduced vascular endothelial growth factor (VEGF) expression. $TGF-\beta$ induction of key target genes involved in bone metastasis, were found to be dependent on Smad3 but not Smad2. Strikingly, whereas knockdown of Smad3 in MDA-MB-231 resulted in prolonged latency and delayed growth of bone metastasis, Smad2 knockdown resulted in a more aggressive phenotype compared to control MDA-MB-231 cells. Consistent with differential effects of Smad knockdown on TGF- β -induced VEGF expression, these opposing effects of Smad2 versus Smad3 could be directly correlated with divergence in regulation of tumor angiogenesis in vivo. Thus, Smad2 and Smad3 differentially affect breast cancer bone metastasis formation in vivo.

Abbreviations

ALK, activin receptor-like kinase; BLI, bioluminescent imaging; BMP, bone morphogenetic protein; CTGF, connective tissue growth factor; EMT, epithelial to mesenchymal transition; GAPDH, glyceraldehyde 3'phosphate dehydrogenase; GFP, green fluorescent protein; IL-11, interleukin 11; miR RNAi, micro RNA interference; MMP, matrix metalloproteinase; N-T control, non-targeting control; PAI-1, plasminogen activator inhibitor 1; PTHrP, parathyroid hormone-related protein; SDS-PAGE, sodium dodecyl sulphate-polyacrylaminde gel electrophoresis; P-Smad, phosphorylated Smad; R-Smad, receptor regulated Smad; Smad, small phenotype and mothers against decapentaplegic related protein; TGF- β , transforming growth factor β ; T β RII, TGF- β type II receptor; VEGF, vascular endothelial growth factor.

Introduction

Metastatic breast cancer is one of the leading causes of death from cancer in women. Transforming growth factor (TGF)- β is frequently overexpressed in human breast tumors and the tumor-associated stroma and its expression correlates with poor prognosis and metastasis [1, 2, 3, 4]. TGF- β is the prototypic member of a large family of evolutionarily conserved pleiotropic cytokines, including three TGF- β isoforms, activins, and bone morphogenetic proteins (BMPs) [5, 6, 7]. TGF- β family members have critical and specific roles during embryogenesis and later in maintaining tissue homeostasis. Perturbations in their signaling pathways have been linked to a diverse set of developmental disorders and diseases, including cancer, fibrosis and auto-immune diseases [8]. These factors signal through specific sets of type I and type II serine/threonine kinase receptors. TGF- β bind to the TGF- β type II receptor (T β RII) which in turn trans-activates the TGF- β type I receptor, also termed activin receptor-like kinase (ALK)5. Activated ALK5 recruits and phosphorylates the receptor-regulated Smads (R-Smads) Smad2 and Smad3. These can then form heteromeric complexes with Smad4, translocate to the nucleus, and control the activation or repression of target genes [9]. Smad2 and Smad3 are also used by activin as downstream signaling mediators [10], whereas BMPs use the R-Smads Smad1, 5, and 8 [11]. Smad2 and Smad3 are highly conserved proteins with 83.9% amino acid sequence identity (Fig. 1A) The major structural difference between Smad2 and Smad3 is in the mad homology 1 domain where Smad2 has two short peptide inserts, amino acids 21-30 and 79-108 [12]. The latter insert imposes steric constraints that prevent Smad2 from binding to DNA [12]. Smad3 on the other hand readily binds DNA in complex with Smad4.

TGF- β has a dual role in tumorigenesis [5]. It inhibits growth of early carcinomas whereas in advanced stages of carcinogenesis TGF- β promotes tumor growth. TGF- β can further stimulate tumor progression and metastasis by inducing epithelial to mesenchymal transition (EMT) and invasion of epithelial cancer cells, [6, 13] and by suppressing anti tumor immune responses [6, 8]. Furthermore, several studies have shown that TGF- β can promote tumor angiogenesis and thereby create a favorable microenvironment for rapid tumor growth and dissemination [13, 14]. In breast cancer bone metastasis target genes of TGF- β are essential for cell homing, establishment of micrometastatic lesions, and in the self-amplifying process of tumor-induced bone resorption [15, 16, 17].

The TGF- β signaling pathway has been extensively studied in cancer patients and in animal models of xenografted tumors and metastasis. In human cancers diffuse phosphorylated Smad2 (P-Smad2) staining has been observed indicative of active TGF- β signaling [18, 19, 20]. Disrupting TGF- β signaling in human breast cancer cells induced tumorigenesis but inhibited invasion and metastasis to lungs after tail vein injection. This was studied by ectopic overexpression of mutated R-Smads or receptors mutated at the R-Smad binding site [21, 22, 23, 24]. Also, when using ALK5 inhibitors in vivo primary tumor growth was inhibited and the number of metastases was reduced [25, 26]. In a model of mouse breast cancer metastasis of 4T1 cells, administration of anti-TGF- β antibody to mice reduced the number of metastasis by 50-60% [27]. In the 4T1 and

the MDA-MB-231 tumor models, systemic administration of a soluble T β RII protein or dominant negative T β RII overexpression, respectively, displayed anti-metastatic effects [16, 28].

Several studies have provided evidence that Smad2 and Smad3 have different transcriptional functions and profiling studies have revealed distinct target genes for Smad2 and Smad3 [29, 30]. Also, whereas mice deficient in Smad2 are embryonic lethal, Smad3 deficient mice are viable [31, 32, 33]. These observations clearly suggest that Smad2 and Smad3 have distinct functions in vivo. In a skin cancer model in mice, homozygous deletion of Smad2 in keratinocytes triggered an EMT phenotype in tumors. This was observed by down-regulation of E-cadherin expression and induction of Vimentin, α -smooth muscle actin, and the E-Cadherin repressor Snail [34]. In contrast, overexpression of activated Smad2/3 was shown to increase cell motility in a squamous skin tumorigenesis models [21]. Nevertheless, the specific functions for Smad2 and Smad3 in breast cancer are not known.

We and others previously reported that silencing Smad4 in breast cancer cells delayed the formation of bone metastasis $in\ vivo\ [19,\ 35]$. To particularly study the contribution of TGF- β signaling in metastasis and explore the exact role of either Smad2 or Smad3, we stably silenced these molecules in an osteotropic clone of the human breast cancer cell line MDA-MB-231. A mouse model of bone metastasis was used to study the differential role of the R-Smads in metastatic progression [35, 36]. Tumor growth and metastasis were quantified $in\ vivo\$ by bioluminescent imaging (BLI). Our results show that, depending on the type of R-Smad silenced the metastatic potential of the human breast cancer cells is differentially and significantly affected.

Results

Specific silencing of Smad2 or Smad3 using miR RNAi

The TGF- β signaling cascade plays crucial roles in breast cancer metastasis. We previously found that silencing Smad4 in MDA-MB-231 cells inhibits bone metastasis formation in vivo [35]. In order to examine direct effects of TGF- β signalling and in particular of the TGF- β R-Smads, we designed and cloned miR RNAi constructs specifically targeting either Smad2 or Smad3. These R-Smads are highly homologous with the exception of the MH1 domain (Fig. 1A) where Smad2 has two additional short peptide inserts compared to Smad3 [12]. The targeting miR RNAi sequences were therefore designed to the additional peptide stretches in the MH1 domain of Smad2 and to the flanking sequences of this region in Smad3. We first examined the efficiency of knockdown of the miR RNAi constructs in a pcDNA 3.1 vector by co-transfection with FLAG-tagged Smad2 or Smad3 in COS cells. A non-targeting (N-T) miR RNAi was used as control. As seen by immunoblot analysis (Fig. 1B lane 4 and 8) both Smad2 and Smad3 were specifically and efficiently silenced by the corresponding miR RNAi. The miR RNAi pcDNA constructs were tested on a specific TGF- β -inducible luciferase reporter in COS and MDA-MB-231 cells, the TGF- β Smad3/Smad4 responsive CAGA-luciferase reporter. The miR RNAi

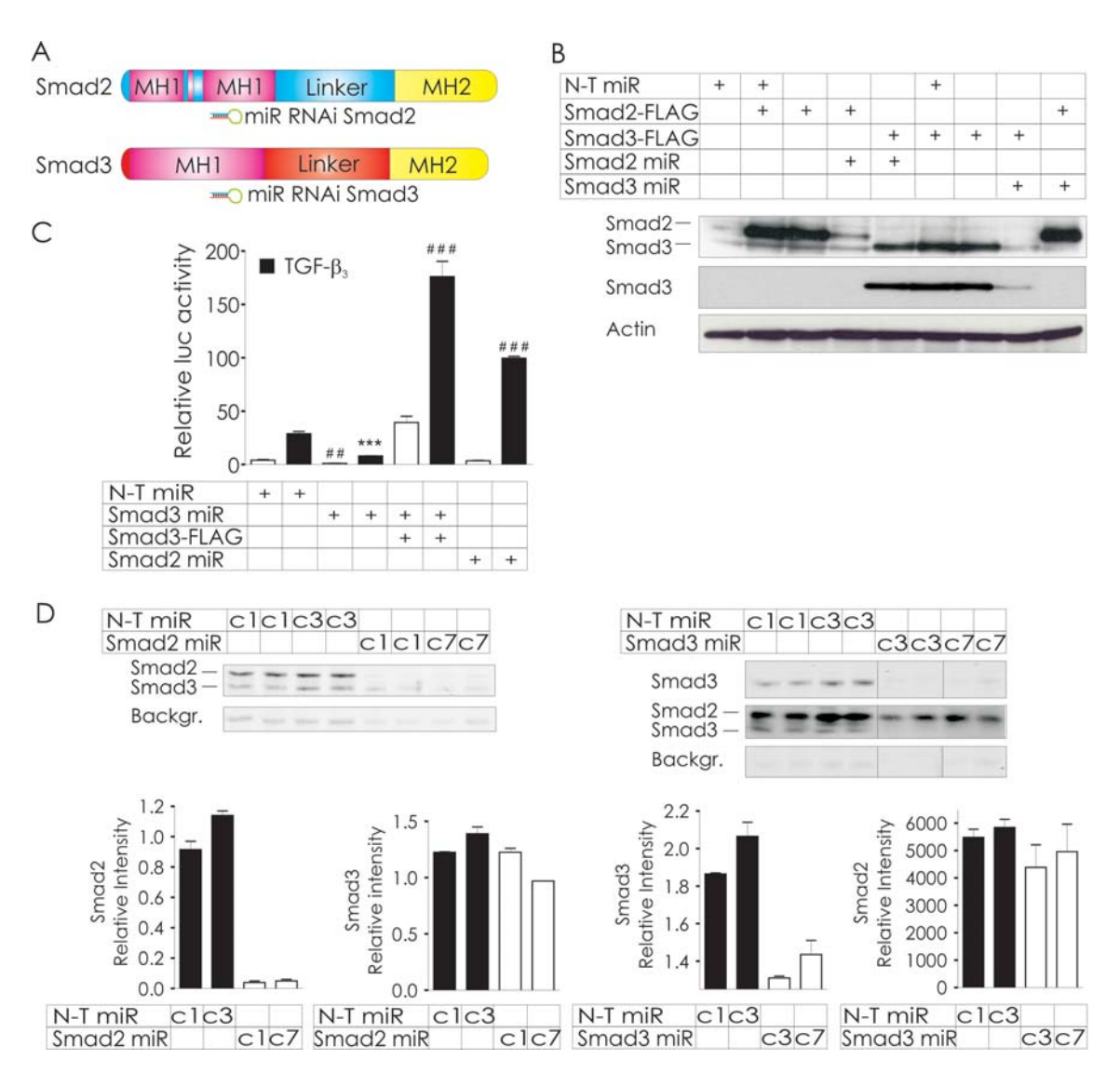


Figure 2.1: Specific silencing of Smad2 or Smad3 using miR RNAi vectors. (A) Schematic illustration of the Smad2 and Smad3 proteins. (B) Immunoblot analysis of Smad2 and Smad3 in COS cells. FLAG-tagged Smad2 or Smad3 were co-transfected with miR RNAi DNA constructs. Protein lysates were separated by SDS-PAGE and analyzed by western blot analysis. Antibodies recognizing Smad3 and Smad2/3 were used. Actin served as a loading control. (C) CAGA-renilla luc reporter transiently co-transfected in COS cells with miR RNAi and Smad3-FLAG constructs in the absence (white bars) or presence (black bars) of TGF- β . Non-targeting (N-T) vs Smad3 miR RNAi #P (P=0.0088), TGF- β -induced control vs TGF- β -induced Smad2 miR RNAi ***P (P=0.0006), TGF- β -induced control vs TGF- β -induced Smad3 miR RNAi with Smad3-FLAG ##P (P=0.0005). (D) Quantitative immunoblot analysis of lentiviral infected MDA-MB-231 clones stably expressing miR RNAi's for Smad2, Smad3 or a N-T control. The relative band intensities of Smad2 or Smad3 are presented below. Values were corrected for equal loading with a non- specific background band. Error bars indicate mean \pm S.D.

targeting Smad3 significantly reduced the TGF-β-induced CAGA-luc activity (Fig. 1C).

The basal level of activity was similarly reduced suggesting that knockdown of Smad3 inhibits autocrine TGF- β signaling. This effect could be rescued by overexpression of Smad3-FLAG. Smad2 miR RNAi significantly potentiated the TGF- β -induced activity (Fig. 1C), suggesting that more Smad3 is accessible at the promoter when Smad2 is eliminated. Neither of the miR RNAi constructs had an effect on the BMP-responsive reporter indicating that the miR RNAi's selectively target Smad2 or Smad3 and not BMP R-Smads or Smad4 (data not shown). The miR RNAi constructs were sub-cloned into lentiviral vectors and MDA-MB-231-luc cells were infected. Several single cell clones stably expressing miR RNAi's were selected and characterized. As shown in Fig. 1D, the stable clones showed efficient knockdown for Smad2 or Smad3. The protein levels of Smad2 in the Smad2 miR RNAi clones were 90-95% reduced. The best knockdown clones with miR RNAi for Smad3 showed a 70-80% reduction of Smad3 protein levels. No cross-targeting was observed for either construct.

Thus, Smad2 and Smad3 are potently and specifically silenced by lentiviral delivered miR RNAi. Binding of TGF- β to its receptor leads to trans-phosphorylation of R-Smads. In order to determine if the levels of phosphorylated Smad2 were elevated in clones silenced for Smad3 and vice versa, we stimulated the stable cell lines with TGF- β (Fig. S1). We further confirmed that a very sufficient knockdown is obtained with the miR RNAi's since no P-Smad2 or P-Smad3 were observed in Smad2 and Smad3 silenced clones, respectively. Furthermore, we found that the level of phosphorylation of one R-Smad was unchanged when the other was silenced. This suggests that the TGF- β -induced activation of R-Smads in MDA-MB-231 cells is non-competitive.

Proliferation of miR RNAi stable clones

Next, we examined if silencing Smad2 or Smad3 would affect *in vitro* cellular proliferation of MDA-MB-231 cells. Relative cell growth profiles for Smad2 miR RNAi, Smad3 miR RNAi, and N-T control miR RNAi stable cell lines were monitored for four consecutive days (Fig. 2A). The Smad3 and the N-T control miR RNAi clones displayed very similar growth curves. The *in vitro* proliferation of the Smad2 miR RNAi clone was significantly lower compared to the other two cell lines (Fig. 2A).

Smad2 and Smad3 are crucial for TGF-β-induced migration

Altered migratory and tumorigenic potential of cancer cells can be simulated by in vitro model systems such as transwell migration. TGF- β induced transwell migration of MDA-MB-231 cells and this was blocked by the ALK5 inhibitor, SB431542 (Fig. 2B). We tested if silencing either Smad2 or Smad3 would affect the TGF- β -induced migratory phenotype of these cells. When Smad2 or Smad3 were knocked down TGF- β failed to stimulate migration. Thus, both Smad2 and Smad3 are critical for TGF- β induced migration of MDA-MB-231 cells in vitro. To characterize the tumorigenic potential of the cells we performed a colony formation assay in soft agar. We observed no difference in the number of colonies formed or in the size of the aggregates (data not shown).

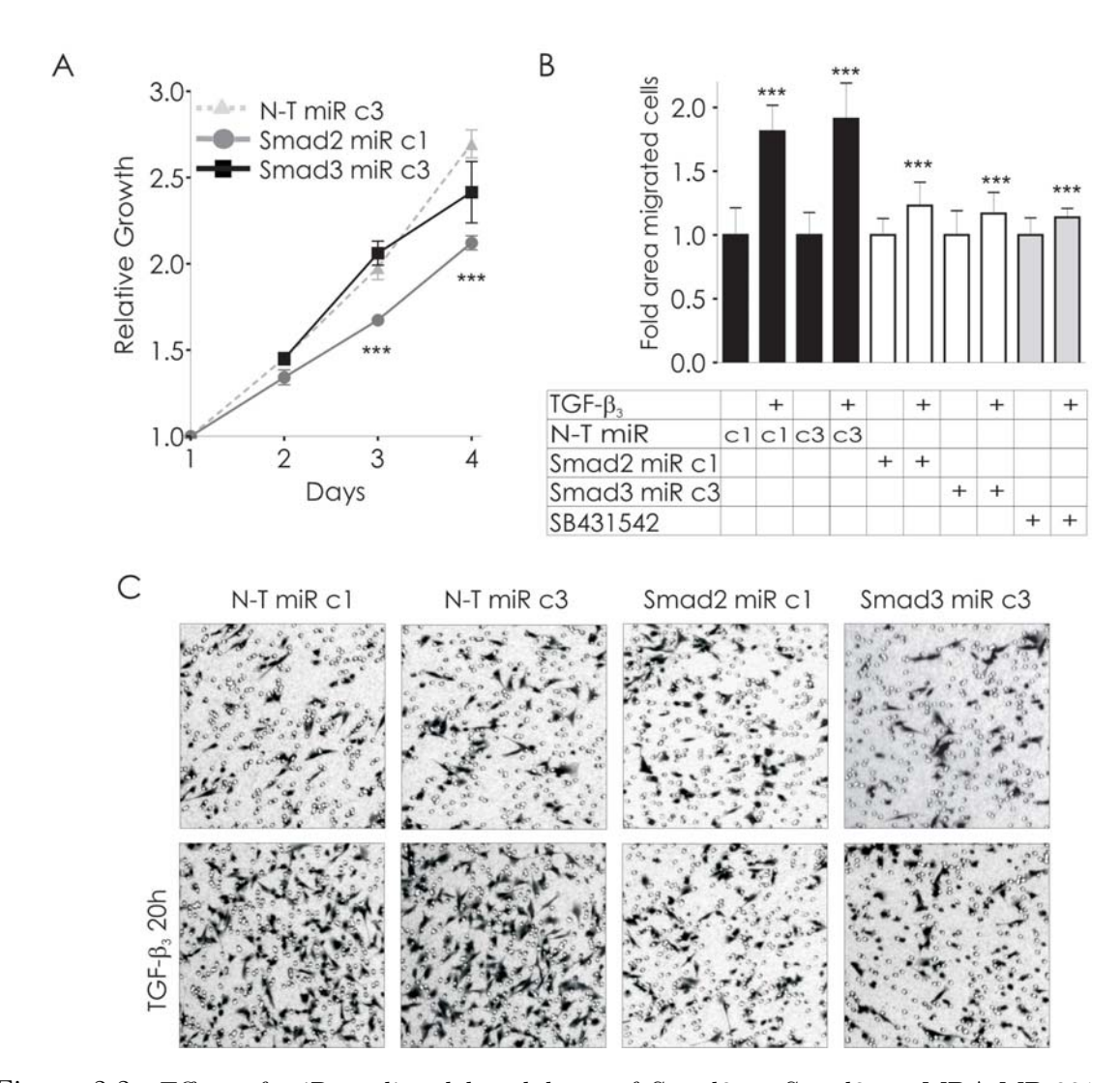


Figure 2.2: Effect of miR-mediated knockdown of Smad2 or Smad3 on MDA-MB-231 cell viability and TGF- β induced migration. (A) Cell proliferation assay of MDA-MB-231 stable clones. The relative growth of Smad2 miR RNAi c1 (circle), Smad3 miR RNAi c3 (square), and N-T miR RNAi c3 (triangle) cells was followed for four consecutive days by measuring mitochondrial activity (MTS assay). Bars represent the mean of four measurements \pm S.D. N-T control and Smad3 miR RNAi versus Smad2 miR RNAi at day 3 and 4 ***P (B) Quantification of transwell migration of MDA-MB-231 cells with or without TGF- β for 20 h. N-T miR RNAi cell lines c1 and c3 (black bars). MiR RNAi silenced Smad2 c1 and Smad3 c3 (white bars). TGF- β induced migration was inhibited in cells treated with the ALK5 inhibitor, SB431542 (grey bars). Values are given as mean \pm S.D. ***P of TGF- β -induced Smad2 miR RNAi (P=0.0006), Smad3 miR RNAi (P=0.0002), and SB431542 (P \leq 0.0001) versus TGF- β -induced N-T control c3. (C) Representative images of MDA-MB-231 stable clones on transwell filters, fixed and stained with crystal violet after migration.

Silencing Smad3 affects TGF- β target genes

Important TGF- β responsive genes involved in the vicious cycle include interleukin (IL)-11, parathyroid hormone-related protein (PTHrP), and connective-tissue growth factor

(CTGF) [15, 16, 35, 37]. We hypothesized that silencing either Smad2 or Smad3 would have an effect on the regulation of TGF- β target genes and perhaps give an indication of the metastatic potential of the cells. In order to look at early target genes of TGF- β we extracted RNA at 6 and 24 hours post stimulation and performed quantitative real time PCR analysis. An increment of IL-11 mRNA levels was seen after 6 hours stimulation with TGF-β in N-T control and Smad2 miR RNAi cells (Fig. 3A). When Smad3 was silenced this induction was significantly inhibited in multiple clones. Also, TGF- β induced PAI-1 expression levels were significantly reduced in Smad3 knockdown cells compared to the control and Smad2 knockdown cells (Fig. 3B). We also examined the TGF- β -induced up-regulation of CTGF (Fig. 3C). CTGF mRNA levels were significantly increased after TGF- β stimulation in the N-T control cells. In Smad2 and Smad3 miR RNAi cells both basal and TGF- β -induced CTGF mRNA levels were reduced. However, the fold induction with $TGF-\beta$ stimulation was comparable to the N-T control. PTHrP mRNA levels were 5 fold induced by TGF- β in all three cell lines (Fig. 3D). To control for off-target effects of the miR RNAi's we used Smad2 and Smad3 shRNAi lentiviral constructs. This resulted in 70-80% knockdown of endogenous protein levels (Fig. S2A). The gene expression analysis was repeated and the effect on TGF- β -induced target genes were confirmed in MDA-BO2 cells stably expressing shRNAi for Smad2 and Smad3 (Fig. S2B-F). Thus, independent approaches for Smad2 or Smad3 knockdown gave nearly identical results indicating that effects of the miR RNAi's are on-target.

Smad2 and Smad3 differentially affect bone metastasis

Our observations in vitro suggest that both R-Smads are necessary for TGF- β -induced migration, whereas Smad3 appears to be more important in the regulation of TGF- β target genes. We evaluated the specific effect of either Smad2 or Smad3 in an experimental mouse model of bone metastasis where osteotropic MDA-MB-231-luc cells were inoculated into the left heart ventricle [35, 36]. This model recapitulates late stages of metastatic progression, namely, survival in the circulation, extravasation, and establishment of metastases at secondary sites. Mice were injected with breast cancer cells stably silenced for either Smad2, Smad3, or a N-T control. Establishment and growth of bone metastatic cells was followed in time with BLI (Fig. 4A). The metastatic growth was plotted as the average total body flux of each experimental group in time (Fig. 4B). Smad2 miR cells showed a significantly more aggressive phenotype compared to both the N-T control and Smad3 miR cell lines (P<0.001 versus Smad3 miR RNAi). In contrast, Smad3 silenced cells displayed a prolonged lag time of tumor growth in the bones (Fig. 4B). This can be more readily observed from the insert of Fig. 4B which demonstrates the tumor growth from day 21 to 35. At this stage the Smad2 silenced metastases are growing at an exponential rate, whereas the Smad3 miR RNAi cells are still in a "lag phase" (P=0.046 Smad2 versus Smad3 miR RNAi). N-T control miR RNAi cells are also starting to grow exponentially at this phase. However, at the end of the experiment there was no significant difference in the total BLI emission from Smad3 miR versus N-T control miR injected mice (Fig. 4B). No significant differences were detected in the

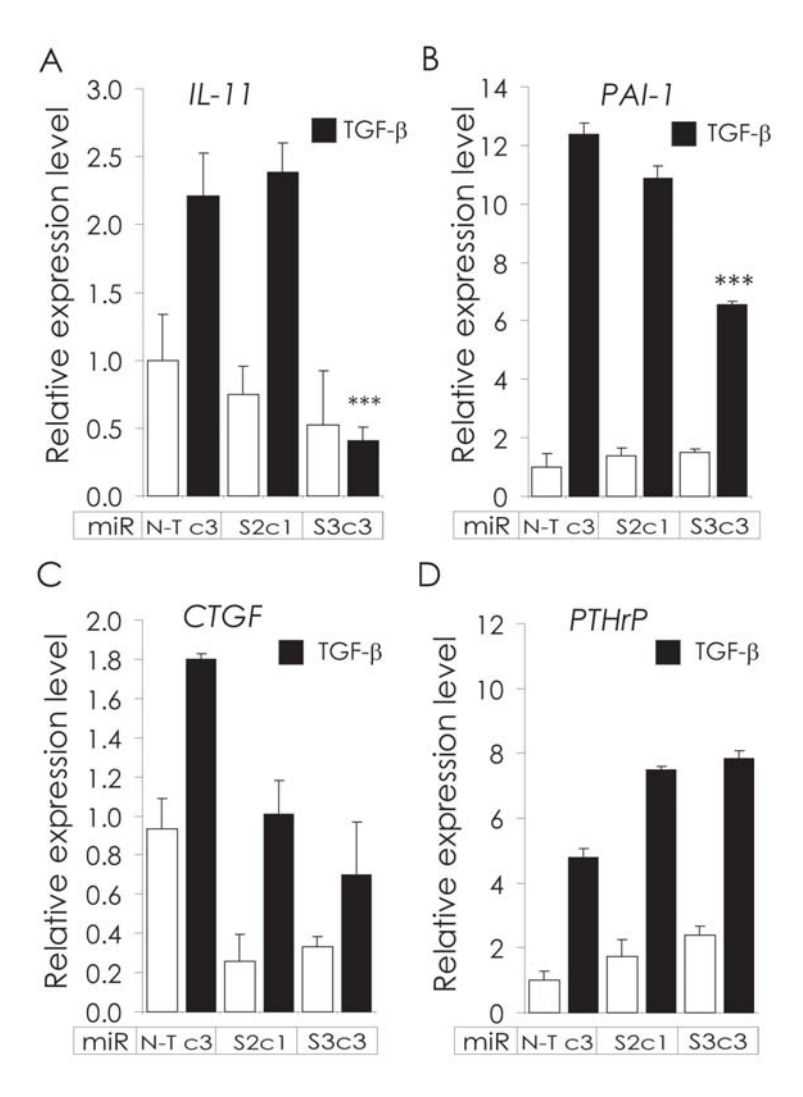


Figure 2.3: Knockdown of Smad2 or Smad3 differentially affects TGF- β -induced target gene expression in MDA-MB-231 cells. Quantitative RT-PCR analysis of TGF- β -induced target genes. Relative expression level of IL-11 (A), PAI-1 (B), CTGF (C), and PTHrP (D) correlated to GAPDH in stable MDA-MB-231 miR RNAi knockdown clones. Cells were stimulated with (black bars) or without (white bars) TGF- β for 6 hours. ***P of stimulated N-T control miR RNAi versus Smad3 miR RNAi cells of IL-11 and PAI-1 mRNA expression levels. Error bars indicate mean \pm S.D.

total number of metastases per animal in each of the three groups (Fig. 4C). However, it appears that there is a tendency for more metastases at an earlier stage in the Smad2 miR RNAi group compared to the N-T and Smad3 miR RNAi groups. Fluorescence imaging was used to visualize the spatial volume of the tumors *in vivo* and examine if the miR RNAi were still actively being expressed. This can be done, since the lentivirally inserted miR RNAi co-cistronically express GFP. As seen in Fig. 4D, showing a Smad2 miR RNAi injected mouse, the bone metastases were highly GFP positive. Radiographies of the same animal reveal the existence of osteolytic bone lesions at the same sites.

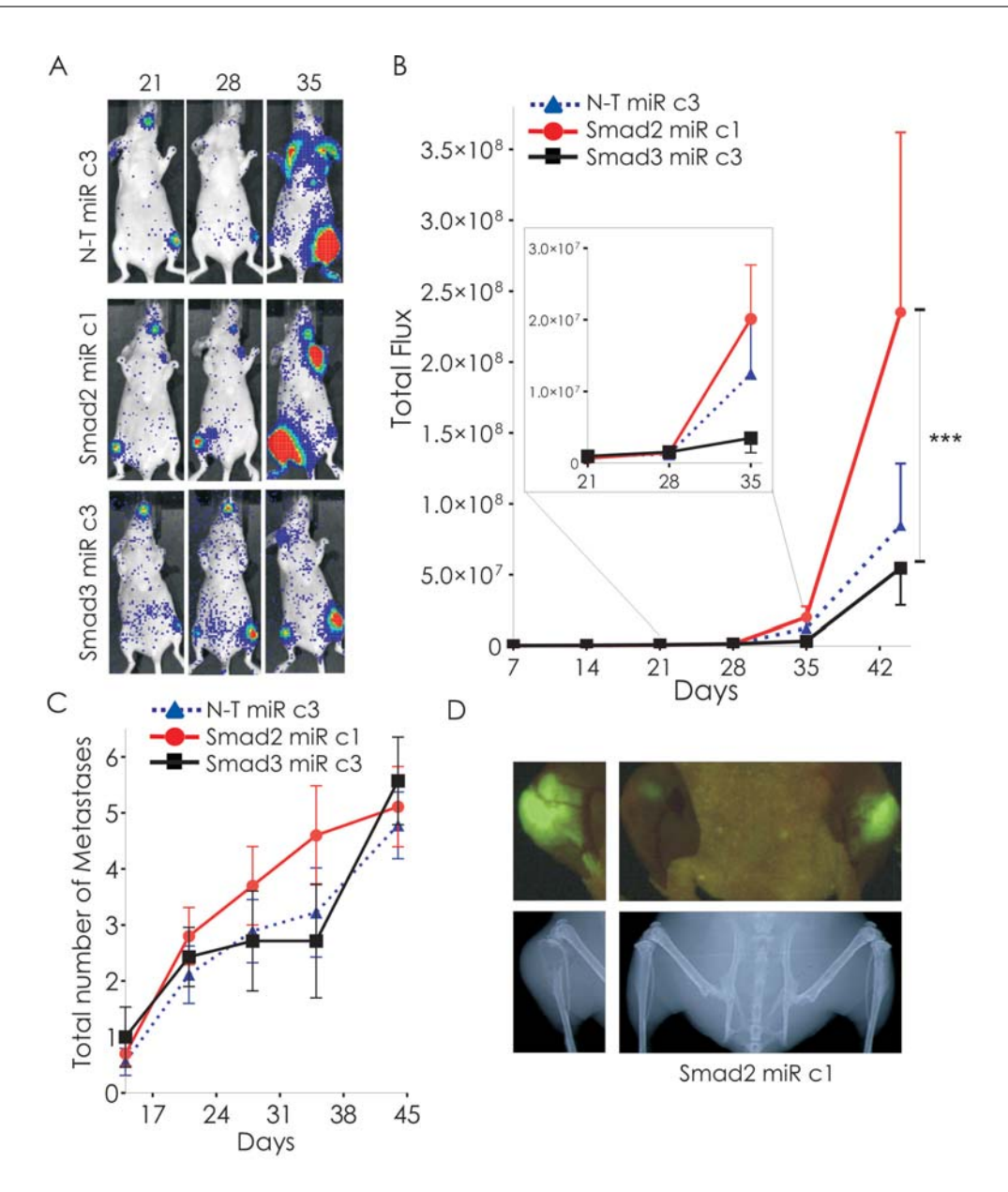


Figure 2.4: Knockdown of Smad2 and Smad3 differentially affect the metastatic profile of MDA-MB-231 cells. (A) *In vivo* BLI at day 21, 28, and 35 of three representative mice injected with MDA-MB-231 luc cells stably expressing N-T control, Smad2, or Smad3 miR RNAi. Ventral images are shown. (B) Average total flux of BLI from each experimental group followed in time. N-T miR RNAi (Triangle, dotted line), Smad2 miR RNAi (circle) Smad3 miR RNAi (square). Asterisks indicate statistically significant difference in total flux at day 45 between Smad2 and Smad3 miR RNAi metastases ***P. Insert show an enlargement of the lower graph from day 21-35. At day 35 Smad2 miR tumor-bearing animals have significantly higher tumor burden compared to Smad3 miR mice *P (P=0.0462). A trend for reduced total flux in Smad3 miR animals compared to N-T control animals was observed (P=0.162). (C) Average amount of metastases per animal in each experimental group. (D) Fluorescent *in vivo* imaging of Smad2 miR RNAi mice and below the corresponding radiographies.

By re-establishment of cell lines from bone marrow aspirates of metastases we found that the stable cell lines were continuously silenced for the respective R-Smad even after *in vivo* passaging (Fig. S3).

Bone metastases are detected as areas of low mineral density where the bone has been extensively resorbed by tumor-induced osteoclasts (Fig. 5). All experimental groups displayed strong osteolytic metastases. In general, the bone metastases were located in the distal femur, proximal tibia, vertebra, mandibula, and os coxae (Fig. 5A arrow heads). When comparing radiographies of mice from different experimental groups, with similar BLI emission, we found no apparent differences in bone destruction (Fig. 5A). This observation was further substantiated by histomorphologic analysis (Fig. 5A and B). Masson-Goldner staining revealed extensive bone loss and nearly complete replacement of the bone marrow with breast cancer cells.

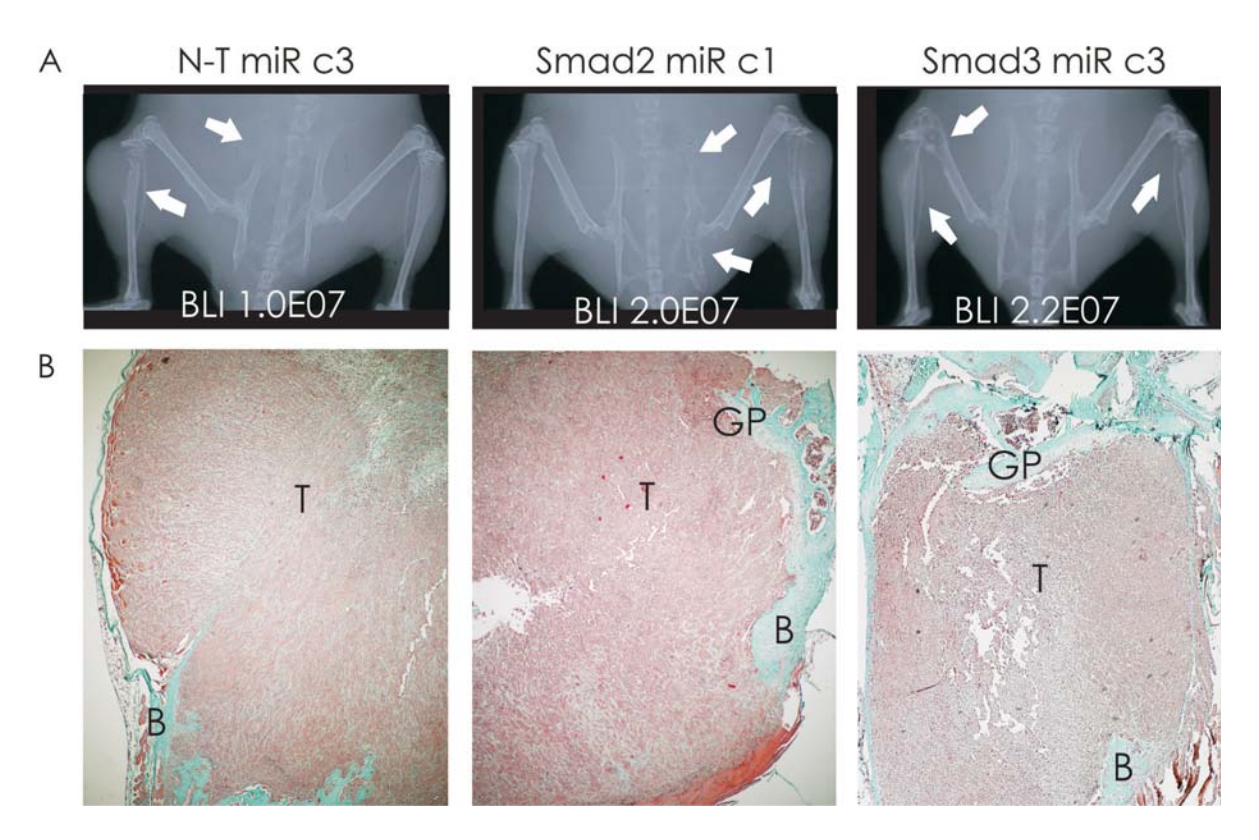


Figure 2.5: Figure 5 Radiographic and histological analysis of bone metastases in mice intracardially injected with MDA-MB-231 cells with or without Smad2 or Smad3 specific knockdown (A) Radiographies of three representative mice with N-T control, Smad2, and Smad3 miR RNAi MDA-MB-231 bone metastases. Arrowheads indicate sites of osteolytic lesions. The BLI values of the tibial regions is given in the lower part of the X-ray. Dorsal side of mice are shown. (B) Histological analysis of tibial proximal metaphyses corresponding to the radiography above. Massons-Goldner trichrome staining of sections to visualize mineralized bone. 4 x magnification. Abbreviations: B, bone; GP, growth plate; T, tumor.

Smad2 and Smad3 differentially regulate angiogenesis

We observed significant differences in metastatic growth of the Smad2 and Smad3 miR RNAi cell lines in vivo. This was seen already at early stages of the metastatic process where the initial growth of Smad3 miR RNAi tumors at the metastatic site was inhibited. At this phase angiogenesis is critically important for metastatic growth [15, 38]. We therefore hypothesized that Smad2 and Smad3 could have differential effects on angiogenesis. VEGF is a key regulator of angiogenesis and directly associated with worse prognosis in patients with invasive breast cancer metastasis [39]. Inhibition of VEGF signaling results in inhibition of breast cancer metastasis [40]. VEGF is a direct TGF- β -induced VEGF production [41, 42].

We therefore analyzed the expression of VEGF-A in the stable miR RNAi clones after 6 and 24 hour TGF- β stimulation (Fig. 6A). TGF- β significantly induced VEGF expression at both time points. Interestingly, when Smad2 was silenced the basal VEGF levels were dramatically increased. In cells lacking Smad3 the TGF- β -induced VEGF expression was lost. We next examined the amount of VEGF secreted in conditioned medium from the miR RNAi clones after TGF- β stimulation (Fig. 6B). In the N-T control miR RNAi cells, TGF- β induced VEGF secretion by 3 fold. In Smad2 miR RNAi cells, 3 fold more VEGF was secreted compared to the N-T control and Smad3 miR RNAi under un-stimulated conditions. This secretion could be further enhanced by TGF- β stimulation. In Smad3 miR RNAi cells TGF- β was unable to induce VEGF production. Thus, the VEGF secretion studies confirmed our transcription profiling results.

To further verify if our observations in vitro would explain the differences in tumor burden in vivo, we visualized the micro-vascular network in the bone metastastatic sections by CD31 (PECAM-1) immunolocalization [36, 38]. Images of the preparations were evaluated by blinded quantification of the micro-vascular density (MVD) and computer analysis of the % capillary area (Figure 6C, 6D, and 6E). Significantly more vascular structures were observed in bone metastases originating from Smad2 miR RNAi cells compared to N-T and Smad3 miR RNAi cells. Furthermore, the expression of the proangiogenic factors hypoxia-inducible factor- 1α and placenta growth factor (PlGF) was enhanced in RNA isolated from Smad2 miR RNAi metastases compared to N-T and Smad3 miR RNAi (Fig. S4). Together these results demonstrate that Smad2 and Smad3 differentially regulate tumor angiogenesis thus, providing an explanation for the observed differences in tumor growth at bone metastatic sites.

Discussion

The concept that the TGF- β signaling pathway plays an important role in tumorigenesis and metastases of breast cancer is well established [5] in clinical and *in vivo* studies [43]. Recently, we and others demonstrated a pro-metastatic role of Smad4 in breast cancer bone metastasis of MDA-MB-231 cells [19, 35]. Due to the nature of Smad4 as a central

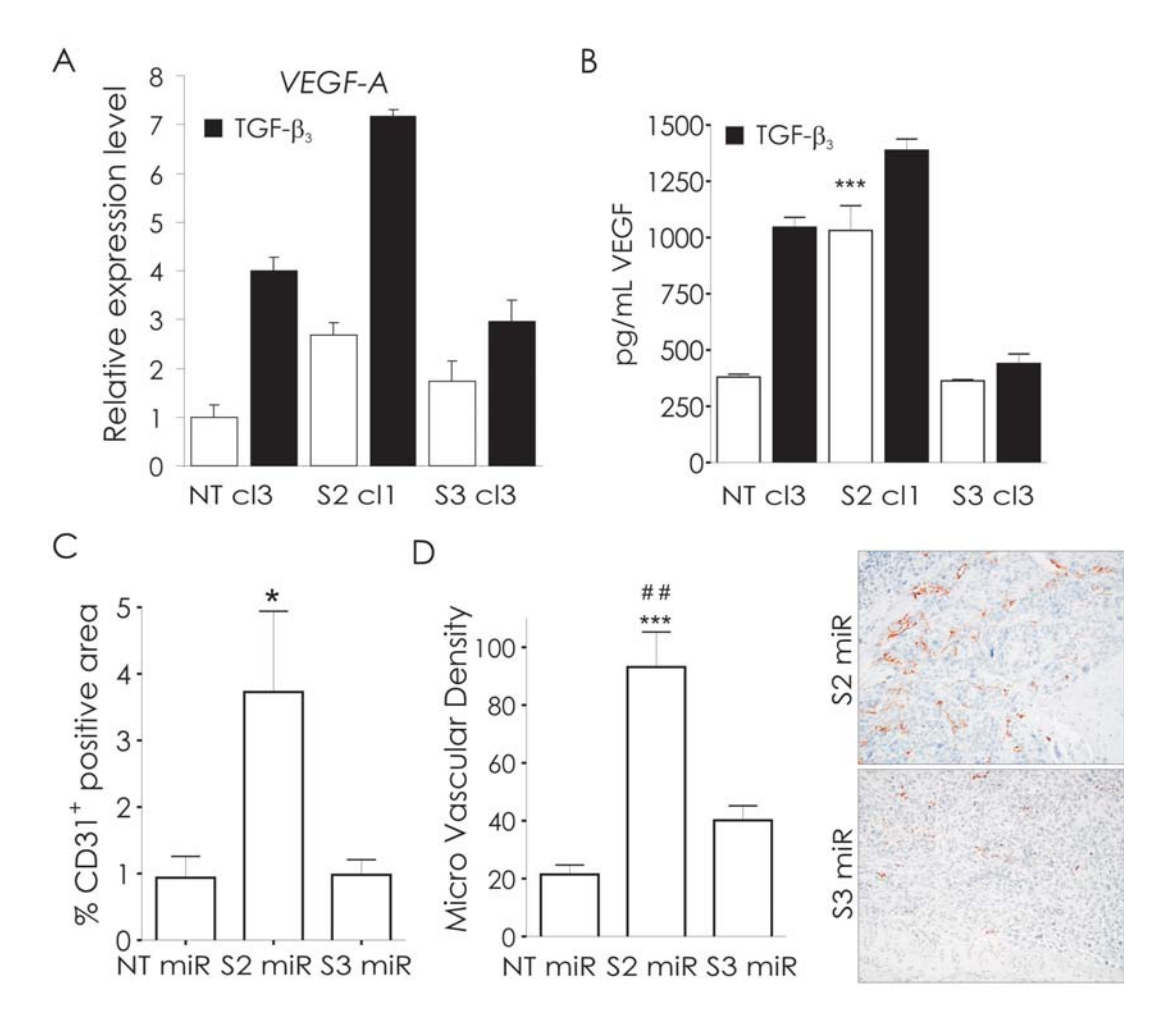


Figure 2.6: Smad2 and Smad3 differentially affect tumor induced angiogenesis (A) Real-time Q PCR analysis of the relative VEGF-A mRNA expression in N-T control, Smad2, and Smad3 miR RNAi MDA-MB-231 clones. GAPDH was used as a housekeeping gene. Cells were stimulated with TGF- β (black bars) or without (white bars) for 6 hours. (B) VEGF protein secretion in the three stable miR RNAi cell lines measured by ELISA. Data is presented at amount of VEGF secreted per ml conditioned medium. ***P of Smad2 miR RNAi versus Smad3 and N-T control miR RNAi cells. Black bars indicate samples stimulated with TGF- β for 15 hours. Error bars indicate mean \pm S.D. (C) Quantification of CD31 staining of bone tumor sections as the % stained area. Asterisks indicate statistically significant more CD31 staining in Smad2 miR RNAi metastases *P versus Smad3 (P=0.033) and N-T control miR RNAi (P=0.046) metastases. (D) Micro vascular density (MVD) in CD31 stained sections from N-T control, Smad2, and Smad3 miR RNAi metastases. A significant higher MVD is observed in Smad2 miR RNAi metastases ***P versus N-T control and $\sharp\sharp\sharp$ P (P=0.0086) versus Smad3 miR RNAi metastases. Error bars indicate mean \pm S.E.M. (D, right) Representative images of CD31 staining in bone sections from mice injected with Smad2 and Smad3 miR RNAi MDA-MB-231 cells.

regulator of both TGF- β and BMP signaling [35, 36] we decided to further study the role of the TGF- β Smad-dependent pathway in breast cancer metastasis by specific

knockdown of either Smad2 or Smad3.

Smad2 or Smad3 expression was eliminated by miR RNAi in the highly aggressive breast cancer cell line MDA-MB-231 and the effect of knockdown was evaluated in several in vitro assays. Furthermore, the metastatic potential of the cells was characterized in a mouse model of bone metastasis [38]. Our in vivo model recapitulates late events in the metastatic cascade including survival in the circulation, homing to bone, extravasation in the bone, and establishment of micrometastatic disease [44]. We show, for the first time, that Smad2 and Smad3 have distinct roles in osteotropic breast cancer. Strikingly, Smad2-silenced MDA-MB-231 cells were considerably more aggressive in vivo than cells silenced for Smad3 or a non-targeting control, despite the fact that they displayed slightly slower proliferation in vitro. In contrast, Smad3 knockdown cells showed a prolonged lag phase of tumor growth in the bone microenvironment. These observations are in line with recent findings by Hoot et al [34] who reported that homozygous deletion of Smad2 potentiated EMT and tumor aggressiveness in a skin cancer model. In these cells a direct up-regulation of critical EMT target genes such as SNAIL and Vimentin was observed along with a reduced E-Cadherin expression in the Smad2^{-/-} skin tumors compared to wild type tumors. We were unable to study the role of EMT in our model which recapitulates later stages of tumorigenesis [35]. Also, Smad2 heterozygous mice displayed accelerated tumor formation and progression compared to wild type control mice [45] and reduced P-Smad2 staining was correlated with a shorter overall survival in patients with stage II breast cancer [20]. Taken together, these observations support our findings regarding the pro-metastatic effects of Smad2 knockdown in breast cancer and suggest that Smad2 has a tumor suppressor role. Bone metastases originating from Smad3 knockdown cells took considerably longer to develop into overt bone lesions. Nevertheless, at the end of the experiment growth of the Smad3 miR RNAi tumors was similar to the N-T control miR RNAi tumors perhaps due to the fact that the knockdown efficiency of Smad3 is not absolute (70-80%). Alternatively, the tumor might induce alternative responses to compensate for the loss of Smad3 as suggested from our findings on HIF-1 α and PIGF expression in Smad3 miR RNAi metastases ([46, 47]). The increased lag phase of bone metastatic growth of Smad3-silenced cancer cells may be explained by altered expression of TGF- β target genes that were no longer responsive to TGF- β when Smad3 was silenced, whereas Smad2 knock down had limited effect on these target genes.

In particular, critical genes involved in the vicious cycle of osteolytic bone metastases, including IL-11, CTFG, and PAI-1, were affected. IL-11 is an important osteolytic factor secreted by the cancer cells to stimulate osteoclastic bone resorption. CTGF and PAI-1 have been reported to stimulate survival in the bone microenvironment through the induction of angiogenesis [15, 48]. Comparable observations were reported for MDA-MB-231 cells knocked down for Smad4 [19, 35].

Blocking the function of endogenous Smad3 in the MCF10A-derived breast cancer cells strongly suppressed formation of metastatic foci in lungs of mice [22, 23], thus supporting our Smad3 findings. In the same study overexpression of a defective binding mutant of Smad3 enhanced malignancy of primary tumors [23]. This is in line with previous findings

where modulation of TGF- β receptors had no effect or even promoted primary tumor growth and at later stages of tumorigenesis significantly reduced invasion and metastatic progression [24, 25, 26, 27]. In our hands, TGF- β -induced migration of MDA-MB-231 cells was dependent on both Smad2 and Smad3. Overexpression of a C-terminal truncated mutant of Smad3 was previously shown to have the same effect on TGF- β -induced migration of MCF10A cells [22]. Taken together these results suggest that Smad3 is critical for stimulation of tumor growth and metastasis.

Angiogenesis is critically important for metastatic growth when the tumor reaches a size that outgrow the normal blood supply [38, 44]. We reckneed that Smad3 miR RNAi metastases grow slower in this phase, which can be explained by a diminished ability to stimulate angiogenesis in the bone metastases. Indeed, significant differences in VEGF-A mRNA expression and VEGF protein secretion were observed. In the Smad3 miR RNAi cell line the TGF- β -induced up-regulation of VEGF was lost, whereas in the Smad2 miR RNAi cell line both VEGF expression and secretion was significantly enhanced. Enhanced angiogenesis was also observed in tumor metastatic sections in Smad2 miR RNAi inoculated animals in agreement with the notion that VEGF directly correlates with the degree of malignancy [39]. In line with our findings, Smad2 was found to mediate secretion of factors with anti-angiogenic properties, whereas Smad3 induced the secretion of pro-angiogenic factors by other epithelial cells [49]. Furthermore, conditioned medium from Smad2 knockout fibroblasts induced proliferation of endothelial cells, whereas medium from Smad3 knockout cells had no effect [49]. These findings support our observations namely that loss of Smad2 potentiate angiogenesis and loss of Smad3 inhibit tumor angiogenesis in breast cancer cells.

We show, for the first time, that Smad2 and Smad3 play distinct roles in breast cancer bone metastasis of MDA-MB-231 cells. Loss of Smad2 significantly increase the metastatic potential whereas loss of Smad3 shows a delayed growth of micro-metastases. These differences can be explained by the distinct roles of Smad2 and Smad3 in tumor-induced angiogenesis. In conclusion, our observations provide evidence that the Smad3 pathway mediates pro-metastatic activities in invasive cells and suggest that Smad2 has tumor suppressor activities. Current therapeutic strategies are aiming at antagonizing the TGF- β receptors thereby completely blocking signaling of both Smad2 and Smad3. Despite the validity of this approach our findings indicate that selectively targeting of Smad3 may lead to more effective therapeutic responses in the treatment of bone metastasis.

Materials and Methods

Cell culture and reagents

MDA-MB-231-luc, MDA-BO2-luc, COS, HEK293T cells were maintained as previously described [35, 36]. Cells were stimulated with TGF- β 3 and BMP6 at 5 and 100 ng/ml, respectively. SB431542 (Tocris bioscience, Bristol, UK) was used at 10 μ M as previously reported [50].

Constructs and cloning

We used BLOCK-iT Pol II micro RNA interference (miR RNAi) technology (Invitrogen, Breda, The Netherlands) for transient and stable knockdown of Smad2 and Smad3 (see supplementary methods for details).

Animals and surgical procedures

4-5 week old female BAlb-c nu/nu mice (Charles River, Maastricht, The Netherlands) were anaesthetized with isofluorane 0.8 l/min and 1×10^5 freshly harvested MDA-MB-231-luc miR RNAi cells in 100 μ l PBS were inoculated into the left heart ventricle (n=10 per group) [35, 36]. Injections were done with 27G syringes. All animal experiments were approved and carried out according to the guidelines provided by the local animal welfare committee.

Statistical analysis

All results are expressed as the mean \pm S.D. or mean \pm S.E.M. as indicated. Two-way ANOVA followed by Bonferronis multiple comparison test and two-tailed Students t-test were used where applicable. P \leq 0.05 was considered to be statistically significant.

Additional procedures

Descriptions of additional experimental procedures used are given in Supplementary Methods.

Acknowledgement

We thank Martine Deckers and Maarten van Dinther for their initial studies and other members of our research group for help and suggestions during the course of this work. We are grateful to Lukas Hawinkels and Hein Verspaget for assistance with VEGF ELISA measurements, Kuber Sampath (Genzyme) for recombinant BMP6 and Ken Iwata (OSI Pharmaceuticals) for recombinant TGF- β 3, and Dr. Philippe Clézardin for the MDA-MB-231 subclone BO2.

References

- [1] S.M. Sheen-Chen, H.S. Chen, C.W. Sheen, H.L. Eng, and W.J. Chen. Serum levels of transforming growth factor $\beta 1$ in patients with breast cancer. *Arch.Surg.*, 136(8):937–940, August 2001.
- [2] V. Ivanovic, N. Todorovic-Rakovic, M. Demajo, Z. Neskovic-Konstantinovic, V. Subota, O. Ivanisevic-Milovanovic, and D. Nikolic-Vukosavljevic. Elevated plasma levels of transforming growth factor-β 1 (TGF-β 1) in patients with advanced breast cancer: association with disease progression. Eur.J. Cancer, 39(4):454–461, March 2003.
- [3] A. Ghellal, C. Li, M. Hayes, G. Byrne, N. Bundred, and S. Kumar. Prognostic significance of TGF β 1 and TGF β 3 in human breast carcinoma. *Anticancer Res.*, 20(6B):4413–4418, November 2000.
- [4] S. Desruisseau, J. Palmari, C. Giusti, S. Romain, P.M. Martin, and Y. Berthois. Determination of $TGF\beta 1$ protein level in human primary breast cancers and its relationship with survival. Br.J. Cancer, 94(2):239–246, January 2006.
- [5] J. Massagué. TGF β in cancer. Cell, 134(2):215–230, July 2008.
- [6] A. Moustakas and C-H. Heldin. Signaling networks guiding epithelial-mesenchymal transitions during embryogenesis and cancer progression. *Cancer Sci.*, 98(10):1512–1520, October 2007.
- [7] B. Schmierer and C.S. Hill. TGFβ-SMAD signal transduction: molecular specificity and functional flexibility. *Nat.Rev.Mol.Cell Biol.*, 8(12):970–982, December 2007.
- [8] K.C. Kirkbride and G.C. Blobe. Inhibiting the TGF- β signalling pathway as a means of cancer immunotherapy. *Expert. Opin. Biol. Ther.*, 3(2):251–261, April 2003.
- [9] P. ten Dijke and C.S. Hill. New insights into TGF-β-Smad signalling. Trends Biochem.Sci., 29(5):265–273, May 2004.
- [10] J.E. Burdette, J.S. Jeruss, S.J. Kurley, E.J. Lee, and T.K. Woodruff. Activin A mediates growth inhibition and cell cycle arrest through Smads in human breast cancer cells. *Cancer Res.*, 65(17):7968–7975, September 2005.
- [11] J. Massague, J. Seoane, and D. Wotton. Smad transcription factors. *Genes Dev.*, 19(23):2783–2810, December 2005.
- [12] S. Dennler, S. Huet, and J.M. Gauthier. A short amino-acid sequence in MH1 domain is responsible for functional differences between Smad2 and Smad3. *Oncogene*, 18(8):1643–1648, February 1999.
- [13] A. Nawshad, D. LaGamba, A. Polad, and E.D. Hay. Transforming growth factor- β signaling during epithelial-mesenchymal transformation: implications for embryogenesis and tumor metastasis. *Cells Tissues. Organs*, 179(1-2):11–23, 2005.
- [14] D. Donovan, J.H. Harmey, D. Toomey, D.H. Osborne, H.P. Redmond, and D.J. Bouchier-Hayes. TGF β -1 regulation of VEGF production by breast cancer cells. *Ann.Surg.Oncol.*, 4(8):621–627, December 1997.
- [15] L.A. Kingsley, P.G. Fournier, J.M. Chirgwin, and T.A. Guise. Molecular biology of bone metastasis. *Mol. Cancer Ther.*, 6(10):2609–2617, October 2007.
- [16] J.J. Yin, K. Selander, J.M. Chirgwin, M. Dallas, B.G. Grubbs, R. Wieser, J. Massagué, G.R. Mundy, and T.A. Guise. TGF-β signaling blockade inhibits PTHrP secretion by breast cancer cells and bone metastases development. J. Clin. Invest, 103(2):197–206, January 1999.
- [17] J.T. Buijs and G. van der Pluijm. Osteotropic cancers: from primary tumor to bone. *Cancer Lett.*, 273(2):177–193, January 2009.

- [18] A. Bruna, R.S. Darken, F. Rojo, A. Ocana, S. Penuelas, A. Arias, R. Paris, A. Tortosa, J. Mora, J. Baselga, and J. Seoane. High TGFβ-Smad activity confers poor prognosis in glioma patients and promotes cell proliferation depending on the methylation of the PDGF-B gene. Cancer Cell, 11(2):147–160, February 2007.
- [19] Y. Kang, W. He, S. Tulley, G.P. Gupta, I. Serganova, C.R. Chen, K. Manova-Todorova, R. Blasberg, W.L. Gerald, and J. Massague. Breast cancer bone metastasis mediated by the Smad tumor suppressor pathway. *Proc.Natl.Acad.Sci.U.S.A*, 102(39):13909–13914, September 2005.
- [20] W. Xie, J.C. Mertens, D.J. Reiss, D.L. Rimm, R.L. Camp, B.G. Haffty, and M. Reiss. Alterations of Smad signaling in human breast carcinoma are associated with poor outcome: a tissue microarray study. *Cancer Res.*, 62(2):497–505, January 2002.
- [21] M. Oft, R.J. Akhurst, and A. Balmain. Metastasis is driven by sequential elevation of H-ras and Smad2 levels. *Nat. Cell Biol.*, 4(7):487–494, July 2002.
- [22] F. Tian, Byfield S. DaCosta, W.T. Parks, S. Yoo, A. Felici, B. Tang, E. Piek, L.M. Wakefield, and A.B. Roberts. Reduction in Smad2/3 signaling enhances tumorigenesis but suppresses metastasis of breast cancer cell lines. *Cancer Res.*, 63(23):8284–8292, December 2003.
- [23] F. Tian, S.D. Byfield, W.T. Parks, C.H. Stuelten, D. Nemani, Y.E. Zhang, and A.B. Roberts. Smadbinding defective mutant of transforming growth factor β type I receptor enhances tumorigenesis but suppresses metastasis of breast cancer cell lines. *Cancer Res.*, 64(13):4523–4530, July 2004.
- [24] J.A. McEarchern, J.J. Kobie, V. Mack, R.S. Wu, L. Meade-Tollin, C.L. Arteaga, N. Dumont, D. Besselsen, E. Seftor, M.J. Hendrix, E. Katsanis, and E.T. Akporiaye. Invasion and metastasis of a mammary tumor involves TGF-β signaling. *Int.J. Cancer*, 91(1):76–82, January 2001.
- [25] S. Ehata, A. Hanyu, M. Fujime, Y. Katsuno, E. Fukunaga, K. Goto, Y. Ishikawa, K. Nomura, H. Yokoo, T. Shimizu, E. Ogata, K. Miyazono, K. Shimizu, and T. Imamura. Ki26894, a novel transforming growth factor-β type I receptor kinase inhibitor, inhibits in vitro invasion and in vivo bone metastasis of a human breast cancer cell line. Cancer Sci., 98(1):127–133, January 2007.
- [26] R. Ge, V. Rajeev, P. Ray, E. Lattime, S. Rittling, S. Medicherla, A. Protter, A. Murphy, J. Chakravarty, S. Dugar, G. Schreiner, N. Barnard, and M. Reiss. Inhibition of growth and metastasis of mouse mammary carcinoma by selective inhibitor of transforming growth factor-β type I receptor kinase in vivo. Clin. Cancer Res., 12(14 Pt 1):4315–4330, July 2006.
- [27] J.S. Nam, M. Terabe, M. Mamura, M.J. Kang, H. Chae, C. Stuelten, E. Kohn, B. Tang, H. Sabzevari, M.R. Anver, S. Lawrence, D. Danielpour, S. Lonning, J.A. Berzofsky, and L.M. Wakefield. An anti-transforming growth factor β antibody suppresses metastasis via cooperative effects on multiple cell compartments. Cancer Res., 68(10):3835–3843, May 2008.
- [28] R.S. Muraoka, N. Dumont, C.A. Ritter, T.C. Dugger, D.M. Brantley, J. Chen, E. Easterly, L.R. Roebuck, S. Ryan, P.J. Gotwals, V. Koteliansky, and C.L. Arteaga. Blockade of TGF-β inhibits mammary tumor cell viability, migration, and metastases. *J. Clin. Invest*, 109(12):1551–1559, June 2002.
- [29] A. Kretschmer, K. Moepert, S. Dames, M. Sternberger, J. Kaufmann, and A. Klippel. Differential regulation of TGF- β signaling through Smad2, Smad3 and Smad4. *Oncogene*, 22(43):6748–6763, October 2003.
- [30] D. LaGamba, A. Nawshad, and E.D. Hay. Microarray analysis of gene expression during epithelial-mesenchymal transformation. *Dev. Dyn.*, 234(1):132–142, September 2005.
- [31] M. Weinstein, X. Yang, C. Li, X. Xu, J. Gotay, and C.X. Deng. Failure of egg cylinder elongation and mesoderm induction in mouse embryos lacking the tumor suppressor Smad2. *Proc.Natl.Acad.Sci.U.S.A*, 95(16):9378–9383, August 1998.

- [32] G.S. Ashcroft, X. Yang, A.B. Glick, M. Weinstein, J.L. Letterio, D.E. Mizel, M. Anzano, T. Greenwell-Wild, S.M. Wahl, C. Deng, and A.B. Roberts. Mice lacking Smad3 show accelerated wound healing and an impaired local inflammatory response. *Nat. Cell Biol.*, 1(5):260–266, September 1999.
- [33] X. Yang, J.J. Letterio, R.J. Lechleider, L. Chen, R. Hayman, H. Gu, A.B. Roberts, and C. Deng. Targeted disruption of SMAD3 results in impaired mucosal immunity and diminished t cell responsiveness to TGF-β. EMBO J., 18(5):1280–1291, March 1999.
- [34] K.E. Hoot, J. Lighthall, G. Han, S.L. Lu, A. Li, W. Ju, M. Kulesz-Martin, E. Böttinger, and X.J. Wang. Keratinocyte-specific Smad2 ablation results in increased epithelial-mesenchymal transition during skin cancer formation and progression. *J. Clin. Invest*, 118(8):2722–2732, August 2008.
- [35] M. Deckers, M. van Dinther, J. Buijs, I. Que, C. Löwik, G. van der Pluijm, and P. ten Dijke. The tumor suppressor Smad4 is required for transforming growth factor β -induced epithelial to mesenchymal transition and bone metastasis of breast cancer cells. Cancer Res., 66(4):2202–2209, February 2006.
- [36] J.T. Buijs, N.V. Henriquez, P.G. van Overveld, G. van der Horst, I. Que, R. Schwaninger, C. Rentsch, P. ten Dijke, A.M. Cleton-Jansen, K. Driouch, R. Lidereau, R. Bachelier, S. Vukicevic, P. Clezardin, S.E. Papapoulos, M.G. Cecchini, C.W. L'owik, and G. van der Pluijm. Bone morphogenetic protein 7 in the development and treatment of bone metastases from breast cancer. Cancer Res., 67(18):8742–8751, September 2007.
- [37] G. van der Pluijm, B. Sijmons, H. Vloedgraven, M. Deckers, S. Papapoulos, and C. Löwik. Monitoring metastatic behavior of human tumor cells in mice with species-specific polymerase chain reaction: elevated expression of angiogenesis and bone resorption stimulators by breast cancer in bone metastases. *J.Bone Miner.Res.*, 16(6):1077–1091, June 2001.
- [38] Y. Kang, P.M. Siegel, W. Shu, M. Drobnjak, S.M. Kakonen, C. Cordon-Cardo, T.A. Guise, and J. Massagué. A multigenic program mediating breast cancer metastasis to bone. *Cancer Cell*, 3(6):537–549, June 2003.
- [39] S. C. Heffelfinger, M. A. Miller, R. Yassin, and R. Gear. Angiogenic growth factors in preinvasive breast disease. *Clin Cancer Res*, 5(10):2867–2876, October 1999.
- [40] J. Matsui, Y. Funahashi, T. Uenaka, T. Watanabe, A. Tsuruoka, and M. Asada. Multi-kinase inhibitor E7080 suppresses lymph node and lung metastases of human mammary breast tumor MDA-MB-231 via inhibition of vascular endothelial growth factor-receptor (VEGF-R) 2 and VEGF-R3 kinase. Clin. Cancer Res., 14(17):5459–5465, September 2008.
- [41] T. Kobayashi, X. Liu, F.Q. Wen, Q. Fang, S. Abe, X.Q. Wang, M. Hashimoto, L. Shen, S. Kawasaki, H.J. Kim, T. Kohyama, and S.I. Rennard. Smad3 mediates TGF-β1 induction of VEGF production in lung fibroblasts. *Biochem. Biophys. Res. Commun.*, 327(2):393–398, February 2005.
- [42] T. Sanchez-Elsner, L.M. Botella, B. Velasco, A. Corbi, L. Attisano, and C. Bernabeu. Synergistic cooperation between hypoxia and transforming growth factor-β pathways on human vascular endothelial growth factor gene expression. *J. Biol. Chem.*, 276(42):38527–38535, October 2001.
- [43] S.K. Leivonen and V.M. Kahari. Transforming growth factor- β signaling in cancer invasion and metastasis. *Int.J. Cancer*, 121(10):2119–2124, November 2007.
- [44] J.T. Buijs, N.V. Henriquez, P.G. van Overveld, G. van der Horst, P. ten Dijke, and G. van der Pluijm. TGF-β and BMP7 interactions in tumour progression and bone metastasis. Clin.Exp.Metastasis, 24(8):609–617, November 2007.
- [45] S.H. Tannehill-Gregg, D.F. Kusewitt, T.J. Rosol, and M. Weinstein. The roles of Smad2 and Smad3 in the development of chemically induced skin tumors in mice. *Vet.Pathol.*, 41(3):278–282, May 2004.

- [46] M. Pàez-Ribes, E. Allen, J. Hudock, T. Takeda, H. Okuyama, F. Viñals, M. Inoue, G. Bergers, D. Hanahan, and O. Casanovas. Antiangiogenic therapy elicits malignant progression of tumors to increased local invasion and distant metastasis. *Cancer Cell*, 15(3):220–231, March 2009.
- [47] J.M.L. Ebos, C.R. Lee, W. Cruz-Munoz, G.A. Bjarnason, J.G. Christensen, and R.S. Kerbel. Accelerated metastasis after short-term treatment with a potent inhibitor of tumor angiogenesis. *Cancer Cell*, 15(3):232–239, March 2009.
- [48] C. Isogai, W.E. Laug, H. Shimada, P.J. Declerck, M.F. Stins, D.L. Durden, A. Erdreich-Epstein, and Y.A. DeClerck. Plasminogen activator inhibitor-1 promotes angiogenesis by stimulating endothelial cell migration toward fibronectin. *Cancer Res.*, 61(14):5587–5594, July 2001.
- [49] T. Nakagawa, J.H. Li, G. Garcia, W. Mu, E. Piek, E.P. B⁵ottinger, Y. Chen, H.J. Zhu, D.H. Kang, G.F. Schreiner, H.Y. Lan, and R.J. Johnson. TGF-β induces proangiogenic and antiangiogenic factors via parallel but distinct Smad pathways. *Kidney Int.*, 66(2):605–613, August 2004.
- [50] M. Petersen, M. Thorikay, M. Deckers, M. van Dinther, E.T. Grygielko, F. Gellibert, A-C. de Gouville, S. Huet, P. ten Dijke, and N.J. Laping. Oral administration of GW788388, an inhibitor of TGF-β type I and II receptor kinases, decreases renal fibrosis. Kidney Int., 73(6):705–715, March 2008.
- [51] A. Nakao, M. Afrakhte, A. Moren, T. Nakayama, J.L. Christian, R. Heuchel, S. Itoh, M. Kawabata, N.E. Heldin, C.H. Heldin, and Dijke P. ten. Identification of Smad7, a TGFβ-inducible antagonist of TGF-β signalling. *Nature*, 389(6651):631–635, October 1997.
- [52] S. Dennler, S. Itoh, D. Vivien, P. ten Dijke, S. Huet, and J.M. Gauthier. Direct binding of Smad3 and Smad4 to critical $TGF\beta$ -inducible elements in the promoter of human plasminogen activator inhibitor-type 1 gene. *EMBO J.*, 17(11):3091–3100, June 1998.
- [53] O. Korchynskyi and P. ten Dijke. Identification and functional characterization of distinct critically important bone morphogenetic protein-specific response elements in the Id1 promoter. *J.Biol.Chem.*, 277(7):4883–4891, February 2002.
- [54] U. Persson, H. Izumi, S. Souchelnytskyi, S. Itoh, S. Grimsby, U. Engström, C-H. Heldin, K. Funa, and P. ten Dijke. The L45 loop in type I receptors for TGF-β family members is a critical determinant in specifying Smad isoform activation. FEBS Lett., 434(1-2):83-87, August 1998.
- [55] L.J. Hawinkels, K. Zuidwijk, H.W. Verspaget, E.S. de Jonge-Muller, W. van Duijn, V. Ferreira, R.D. Fontijn, G. David, D.W. Hommes, C.B. Lamers, and C.F. Sier. VEGF release by MMP-9 mediated heparan sulphate cleavage induces colorectal cancer angiogenesis. *Eur.J. Cancer*, 44(13):1904–1913, September 2008.
- [56] N.V. Henriquez, P.G. van Overveld, I. Que, J.T. Buijs, R. Bachelier, E.L. Kaijzel, C.W. L'owik, P. Clezardin, and G. van der Pluijm. Advances in optical imaging and novel model systems for cancer metastasis research. *Clin.Exp.Metastasis*, 24(8):699–705, October 2007.

Supplementary Material

Supplementary Figures

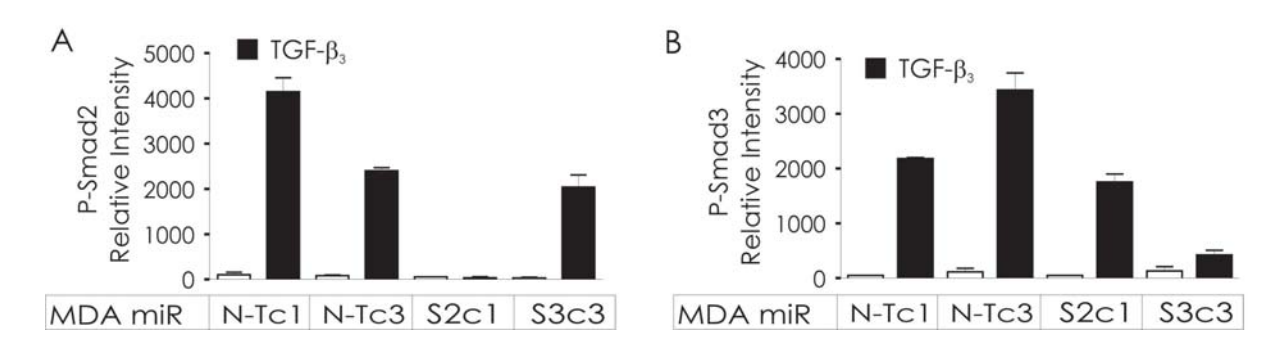


Figure 2.7:

Supplementary figure 1.

Relative densitometric analysis of western blot for P-Smad2 (A) and P-Smad3 (B). Cells were stimulated for 1 hour with TGF- β (black bars) where indicated. Protein levels were normalized with a non-specific background band.

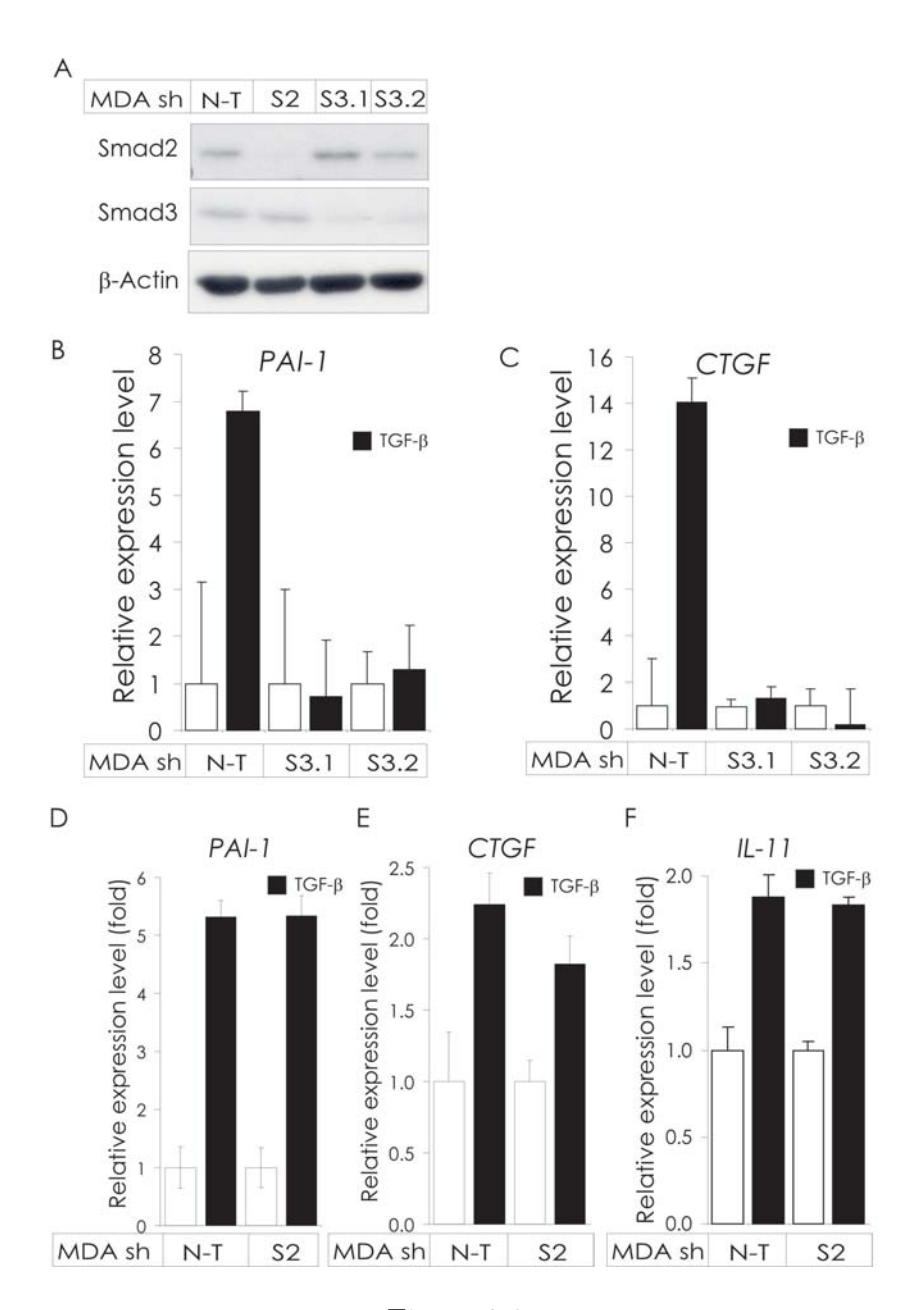


Figure 2.8:

Supplementary figure 2. (A) Immunoblot analysis of Smad2 and Smad3 protein levels in MDA-B02 cells stably knocked down for Smad2 or Smad3. Control cells were infected with a non-targeting (N-T) control shRNAi vector. MDA-B02 cells were lentivirally infected with specific shRNAi expressing vectors and selected for uptake of the shRNA vector by culturing the cells with puromycin. Real-time analysis of PAI-1 (B) and CTGF (C) in Smad3 shRNAi MDA-B02 cells and PAI-1 (D), CTGF (E), and IL-11 (F) in Smad2 shRNAi MDA-B02 cells after 6 hours TGF- β stimulation (black bars).

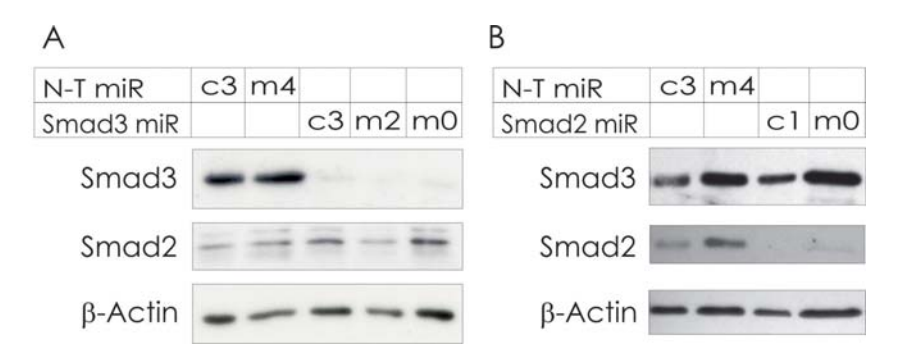


Figure 2.9:

Supplementary figure 3. Immunoblot analysis of MDA-MB-231 cells stably expressing miR RNAi for N-T control and the cell line m4 originating from a N-T control miR RNAi metastasis. Smad3 miR RNAi cells and the re-established cell lines m0 and m2 both originating from Smad3 miR RNAi metastases.

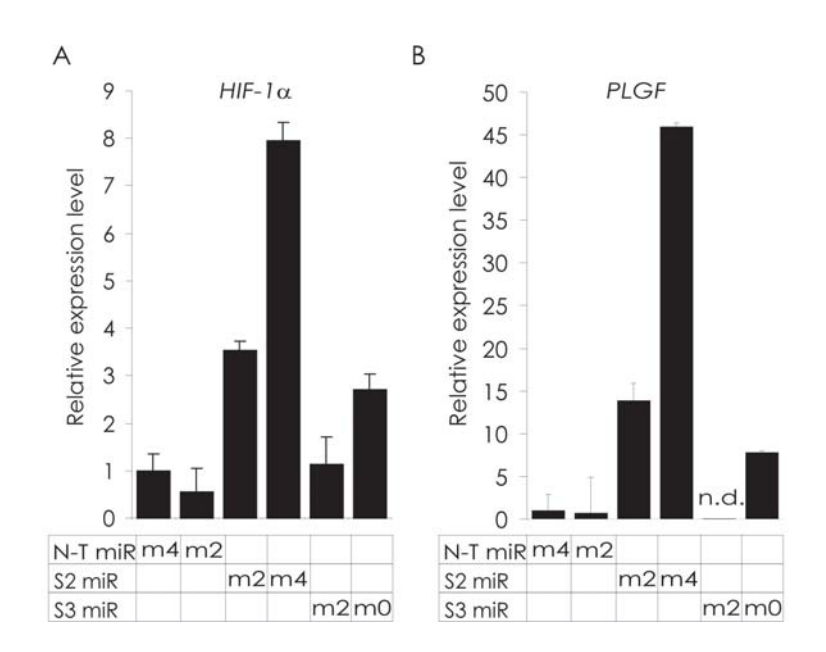


Figure 2.10:

Supplementary figure 4. Real-time PCR analysis of hypoxia inducible factor 1 α (HIF-1 α) and placenta growth factor (PlGF) in bone metastasis from mice inoculated with N-T control, Smad2 miR RNAi or Smad3 miR RNAi breast cancer cells.

Supplementary Methods

Constructs and cloning

We used the BLOCK-iT Pol II micro RNA interference (miR RNAi) technology (Invitrogen) for transient and stable silencing of Smad2 and Smad3. The targeting sequence for Smad2 was 5'-ACC AAG CAC TTG CTC TGA AAT-3' and for Smad3, 5'-AGA ACG TCA ACA CCA AGT GCA-3'. The non-targeting (N-T) sequence was 5'-ACG TCT CCA CGC AGT ACA TTT-3'. Oligonucleotides were cloned into pcDNA6.2 GW-EmGFPmiR expression vector which co-cistronically express the miR RNAi and emerald green GFP (EmGFP) and transferred to the pLenti6/V5-DEST vector (Invitrogen). Cells were lentivirally infected and single cell clones selected with 5 ng/ml blasticidin (Invitrogen). We used shRNAi targeting Smad2 or Smad3 from the MISSION lentiviral library (Sigma). After lentiviral infection transfectants were selected with 1 μ g/ml puromycin. ShRNAi for Smad2 was TRCN-0000010477 and for Smad3 TRCN-0000020011 and TRCN-0000020012. As controls a non-targeting sequence and a GFP targeting sequence were used. The N-terminally tagged Flag-Smad2 and Flag-Smad3 expression plasmids were previously described [51].

Cell transfection and cell viability assay

Cells were seeded in 24-well plates and the following day transiently co-transfected with miR RNAi constructs and CAGA 12-Renilla or the BRE-Renilla luciferase reporter constructs in which the firefly was replaced with Renilla luciferase ([52, 53] and unpublished data). The ratio of reporter construct versus miR RNAi was 1:6. We used Lipofectamine (Invitrogen) or FugeneHD (Roche) according to the manufacturers protocol. Two days after transfection, cells were stimulated for 15 hours with the respective ligands and the relative Renilla/firefly luciferase activity was measured. CMV-firefly luciferase was used to control transfection efficiency. Each transfection was done in triplicate and representative experiments are shown. Cell viability was performed as previously described [50].

Western blot analysis

Proteins were separated on SDS-PAGE and subjected to Western blotting using standard techniques [50]. Antibodies recognizing phosphorylated Smad2 (P-Smad2) and phosphorylated Smad 1/5 (P-Smad1/5) are described in [54]. P-Smad1/3 was a kind gift from Dr. E. Leof (Rochester, Minnesota, USA). Smad2/3 (BD transduction laboratories, Belgium), Smad3 (Zymed, CA, USA or AbCam, MA, USA), and -Actin (AC-15, Sigma, Netherlands). Secondary antibodies were either HRP or near infrared (NIR) labeled and detection performed with chemiluminescence or fluorescence scanning on the LI-COR Odyssey.

Quantitative real-time PCR

Total RNA and cDNA synthesis were performed as previously described [50]. Samples were run in triplicates for each primer set. Gene expression levels were assessed as the threshold cycle (Ct) values of the target gene and reference gene normalized to GAPDH ($\Delta\Delta Ct$ method). Relative expression levels are presented as mean $\pm S.D$. The following human primers were used; CTGF, forward 5'-TTG CGA AGC TGA CCT GGA AGA GAA-3' and reverse 5'-AGC TCG

GTA TGT CTT CAT GCT GGT-3'; PAI-1 forward 5'-TCT TTG GTG AAG GGT CTG CT-3' and reverse 5'-CTG GGT TTC TCC TCC TGT TG-3'; HIF-1 α forward 5'-GCA AGC CCT GAA AGC-3' G and reverse 5-GGC TGT CCG ACT TTG A-3'; PIGF 5'-ACG TGG AGC TGA CGT TCT CT-'3 and reverse 5'-CAG CAG GAG TCA CTG AAG AG-'3; IL-11 5'-ACT GCT GCT GCT GAA GAC TC-3' and reverse 5'-CCA CCC CTG CTC CTG AAA TA-3'; PTHrP forward 5'-ACC TCG GAG GTG TCC CCT AAC-3' and reverse 5'-TCA GAC CCA AAT CGG ACG-3'; VEGF-A forward 5'-AGC CTT GCC TTG CTG CTC TA-3' and reverse 5'-GTG CTG GCC TTG GTG AGG-3'.

Transwell migration

Transwell migration was performed in 24 well plates with filter inserts of a pore size of 0.8 μ m (Corning Costar, CA, USA). 30.000 pre-starved cells were seeded in the upper chamber in 200 μ l medium. 300 μ l medium with or without stimuli was added to the lower chamber. Experiments were done in triplicates. Cells were fixed after 20 hours with 4% paraformaldehyde and stained with 0.1% crystal violet. Pictures were acquired with phase-contrast microscopy at 10 x magnification. Three fixed positions were imaged of each membrane. The area covered by cells was quantified by binary image analysis using the NIH/ImageJ software.

VEGF secretion

VEGF secretion in conditioned media from stable miR RNAi MDA-MB-231 cells was analyzed by quantitative sandwich ELISA. Media were harvested 15 hours with or without stimulation with TGF- β and the analysis was performed as previously described [55].

In vivo imaging and Radiography

Metastatic tumor growth was followed weekly by live BLI with the IVIS 100 (Caliper Life Sciences) as previously described [35, 36]. The BLI signal intensity was quantified as the sum of photons within a region of interest given as the total flux (photons per second). Fluorescence-based imaging of EmGFP was measured with the CRi Maestro FLEX system [56] (Cambridge Research Instrumentation). The skin was carefully removed from the tibial regions prior to imaging. GFP emission was measured at 550 nm with an automatically estimated scan time of 360 ms. Radiographs were taken after *in vivo* fluorescent measurements as previously described [35, 36].

Establishment of in vitro cell lines from metastases

Whole bone metastases were surgically excised for histochemical analysis and *in vitro* tumor cell growth. Cell lines were established by removal of the tibial diaphysis and aspirating the metaphysis with cell culture medium. Bone marrow aspirates were plated in tissue culture asks and selection with neomycin was initiated the following day. This selects only for MDA-MB-231 cells expressing the CMV-luciferase construct enabling us to determine if cells have retained Smad2 or Smad3 knockdown caused by the expression of the miR RNAi.

RNA isolation from bone metastases

Whole bone metastases were surgically excised for RNA extraction. Samples were pulverized with a hammer under sterile conditions and processed as previously described [35].

Histochemistry and immunohistochemistry

Tissue samples were embedded in paraffin and 5 μ m sections were stained with the Masson-Goldners method to visualize mineralized bone [35, 36]. The micro-vasculature in metastases was visualized by CD31 staining using standard techniques [37] and images were acquired with phase-contrast microscopy. The area covered by CD31 positive staining was quantified with image analysis and quantification of the micro vascular density was done by counting vessels in a given area.